DOI: 10.1002/ejoc.200500431

The Effect of a Host–Guest Hydrogen Bond on the Inclusion of Alcoholic Guests in the Host Cavities of Cholamide

Nungruethai Yoswathananont,[a] Kazuki Sada,[b] Kazunori Nakano,[c] Kazuaki Aburaya,[a] Masashi Shigesato,[a] Yukio Hishikawa,[a] Kanae Tani,[a] Norimitsu Tohnai,[a] and Mikiji Miyata*[a]

Keywords: Alcohols / Amides / Host–guest systems / Hydrogen bonds / Inclusion compounds

Fifty eight inclusion crystals of cholamide (CAM) with aliphatic alcohols have been systematically investigated by X-ray crystallography. The host frameworks of the inclusion crystals can be categorized into three structural types: bilayer, herringbone, and crossing structures. Most of the guests are included in bilayer structures, which can be further divided into four sub-types. The host frameworks isomerize depending on the size and shape of the guest molecules. This dependence is clearly evaluated by the relationship between the volume of the guest molecules and the packing coefficient of the void space in the host frameworks. Although the host frameworks with the cavities and the structural isomerization are very similar to those of the inclusion crystals of cholic acid (CA), the inclusion behavior of aliphatic alcohols in the two hosts is completely different: fifty four alcohols can be included in the bilayer-type structures of CAM, but only two in those of CA. This is attributed to their different functional groups, which lead to different hydrogen-bond networks with the guest alcohols. The result in the two hosts is a good example to understand the effect of host–guest hydrogen bonds on guest inclusion in cavities that are identical in size and shape.

Introduction

Nanoporous, crystalline organic compounds constructed by hydrogen bonds have attracted much attention in the field of supramolecular chemistry.[1,2] One of their significant features is the flexibility of the host frameworks with nanosize pores. Recent extensive structural studies have revealed that most host compounds change their host frameworks in response to guests acting as a template.[3–13] In particular, hydrogen bond proton donating guests, such as water, alcohols, amines, and carboxylic acids, often form host–guest hydrogen bonds, which means that they form different host frameworks to those with apolar guests.[12,13] The importance of the recombination of host–guest hydrogen bonds has also resulted in the resolution of racemates and the separation of isomers using inclusion compounds.[14]

Recently, we have reported that cholamide (3α,7α,12α-trihydroxy-5β-cholamide, CAM, Scheme 1), the primary amide of cholic acid (3α,7α,12α-trihydroxy-5β-cholanic acid, CA, Scheme 1), forms inclusion crystals with a wide range of organic compounds.[15] In particular, fifty or more aliphatic alcohols can be included in CAM crystals.[15e] X-ray crystallographic studies of these compounds revealed that several inclusion crystals of CAM have a bilayer structure with a one-dimensional cavity,[15e] as in the case of CA crystals that have been systematically investigated.[16] On the other hand, only two aliphatic alcohols can be included in CA bilayer crystals,[16c] and most alcohols act rather as good solvents for the formation of inclusion compounds of CA with aprotic guests.[16d] This difference between the inclusion in CAM and CA crystals prompted us to investigate extensively the crystal structures of CAM with aliphatic alcohols. In this report, we describe our extensive structural investigations, which reveal the effect of the host–guest hydrogen bonds on the inclusion of alcoholic guests.

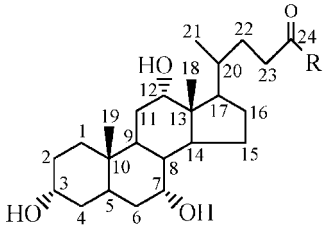

R = NH_2 Cholamide (**CAM**)
R = OH Cholic Acid (**CA**)

Scheme 1. Molecular structures of CAM and CA.

[a] Department of Materials and Life Science, Graduate School of Engineering, Yamadaoka, Suita, Osaka University, Osaka 565-0871, Japan
[b] Department of Chemistry and Biochemistry, Graduate School of Engineering, Kyushu University, 6-10-1 Hakozaki, Higashi-ku, Fukuoka 812-8581, Japan
[c] Nagoya Municipal Industrial Research Institute, 3-4-41 Rokuban, Atsuta-ku, Nagoya 456-0058, Japan
Supporting information for this article is available on the WWW under http://www.eurjoc.org or from the author.

Results and Discussion

General Scope of CAM Inclusion Crystals with Alcohols

Fifty six new crystal structures of CAM with aliphatic alcohols (Scheme 2, including racemic and *cis*/*trans* mixtures) were determined by X-ray crystallography, while two crystal structures, CAM·**4** and CAM·**9**, have already been reported.[15e] The crystallographic parameters are summarized in Table S1 (Supporting Information), and typical crystal structures are depicted in Figure 1. The crystals have 1:2, 1:1, or 2:1 host/guest molar ratios, and are categorized into three structural types: bilayer, herringbone, and crossing structures. The latter two types are new. Table 1 shows the relationship between the number of included guests and structural types with the host/guest ratios. The host/guest ratios are dependent mainly on the number of carbons in the guest molecules: two small guests (C1 and C2) form inclusion crystals with 1:2 host/guest ratios, nine larger guests (C6 or more) with 2:1 ratios, and forty seven middle-size guests (C3–C8) with a 1:1 ratio. This table also indicates that the bilayer structure is ubiquitous, but that the herringbone and crossing structures are quite rare. The features of these host frameworks with the host cavities and the hydrogen-bond networks are discussed further below.

R-OH

Guest	R	Guest	R
1	CH_3	**24**	$CH_3CH_2(CH_3)CH(CH_3)CH$
2	CH_3CH_2	**25**	$(CH_3)_2CHCH_2(CH_3)CH$
3	$CH_3(CH_2)_2$	**26**	$CH_3CH_2((CH_3)_2CH)CH$
4	$(CH_3)_2CH$	**27**	$(CH_3)_3C(CH_2)_2$
5	$(CH_3)_2CHCH_2$	**28**	$(CH_3)_3C(CH_3)CH$
6	$(CH_3)_3C$	**29**	$CH_3CH_2(CH_3CH_2)CHCH_2$
7	$(CH_3)(COCH_3)CH$	**30**	$CH_3(CH_2)_5$
8	$CH_3(CH_2)_3$	**31**	$CH_3(CH_2)_3(CH_3)CH$
9	$(CH_3CH_2)(CH_3)CH$	**32**	$CH_3(CH_2)_2(CH_3CH_2)CH$
10	$CH_3CH_2(CH_3)CHCH_2$	**33**	$(CH_3)_3CCH_2(CH_3)CH$
11	$(CH_3)_2CH(CH_2)_2$	**34**	$((CH_3)_2CH)_2CH$
12	$CH_3CH_2(CH_3)_2C$	**35**	$CH_3(CH_2)_3(CH_3)CHCH_2$
13	$(CH_3)_2CH(CH_3)CH$	**36**	$CH_3(CH_2)_6$
14	$(CH_3)_3CCH_2$	**37**	$CH_3(CH_2)_4(CH_3)CH$
15	$CH_3(CH_2)_4$	**38**	$CH_3(CH_2)_3(CH_3CH_2)CH$
16	(*R*)-$CH_3(CH_2)_2(CH_3)CH$	**39**	$(CH_3CH_2CH_2)_2CH$
17	(*S*)-$CH_3(CH_2)_2(CH_3)CH$	**40**	$CH_3(CH_2)_7$
18	$CH_3(CH_2)_2(CH_3)CH$	**41**	$CH_3(CH_2)_5(CH_3)CH$
19	$(CH_3CH_2)CH$	**42**	$CH_3(CH_2)_4(CH_3CH_2)CH$
20	$CH_3(CH_2)_2(CH_3)CHCH_2$	**43**	$CH_3(CH_2)_8$
21	$CH_3CH_2(CH_3)CH(CH_2)_2$	**44**	$(CH_3(CH_2)_3)_2CH$
22	$(CH_3)_2CH(CH_2)_3$	**45**	$CH_3(CH_2)_9$
23	$CH_3(CH_2)_2(CH_3)_2C$	**46**	$CH_3(CH_2)_4(CH_3(CH_2)_3)CH$

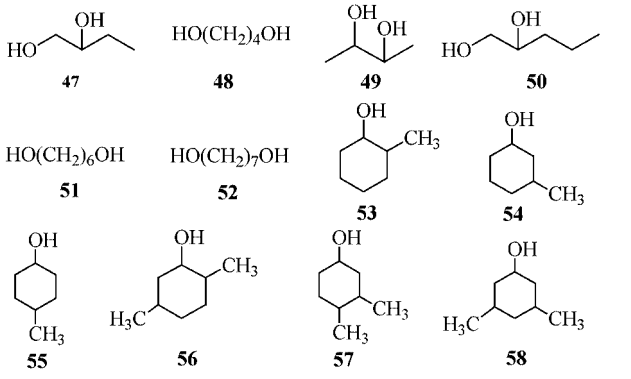

Scheme 2. Aliphatic alcohols included in CAM.

Bilayer Structure

Figure 1 (a–d) shows four typical bilayer structures composed of two sets of hydrophilic and lipophilic layers. The host frameworks can be further classified into four subtypes (α-*trans*, α-*gauche*, β-*trans*, and β-*gauche*) on the basis of the conformation of the side-chain; *trans* and *gauche* are assigned from the torsion angle (ψ) of C17–C20–C22–C23 (Figure 2) and the interdigitation manner, whereas α and β are due to the lipophilic layers (Figure 3). Guest molecules are included in the one-dimensional cavity in the lipophilic layer. Figure 4 shows the typical cross-sectional views sliced perpendicular to the axis of the channel using MODRASTE.[17] The β-*trans* structure type has a larger cavity than the others, while elliptical cross-sections of the cavities are inherent in these types. In the hydrophilic layers, the host molecules are connected by hydrogen-bond networks, as shown in Figure 5. The hydrogen-bond lengths are summarized in Table S2 (Supporting Information). All the crystals have host–host cyclic hydrogen-bond networks of the type ···OH[C(7)]···OH[C(3)]···OH[C(12)]···O=C–NH_2[C(24)]···, and the adjacent cyclic networks, except the case of **39**, are bridged by alcoholic guest molecules. The bridges are classified into two types of sequence: type I (O=C–NH_2[C(24)]···OH[guest]···O=C–NH_2[C(24)]) and type II (O=C–NH_2[C(24)]···OH[guest]···OH[C(12)]). Only **39** gives a type III network, in which the guest molecule is attached to the host–host cyclic hydrogen-bond network. All the network types are independent of the host framework types, as shown in Table S1 (Supporting Information).

Table 1. Numbers of included guests in structural types.

Structural type (host/guest ratio)	Carbon numbers of guest molecules										
	C1	C2	C3	C4	C5	C6	C7	C8	C9	C10	Total
Bilayer (1:2)		1									1
Bilayer (1:1)			2	6	11	13	8	4			44
Bilayer (2:1)						1	2	2	2	2	9
Herringbone (1:2)	1										1
Herringbone (1:1)				2							2
Crossing (1:1)							1				1

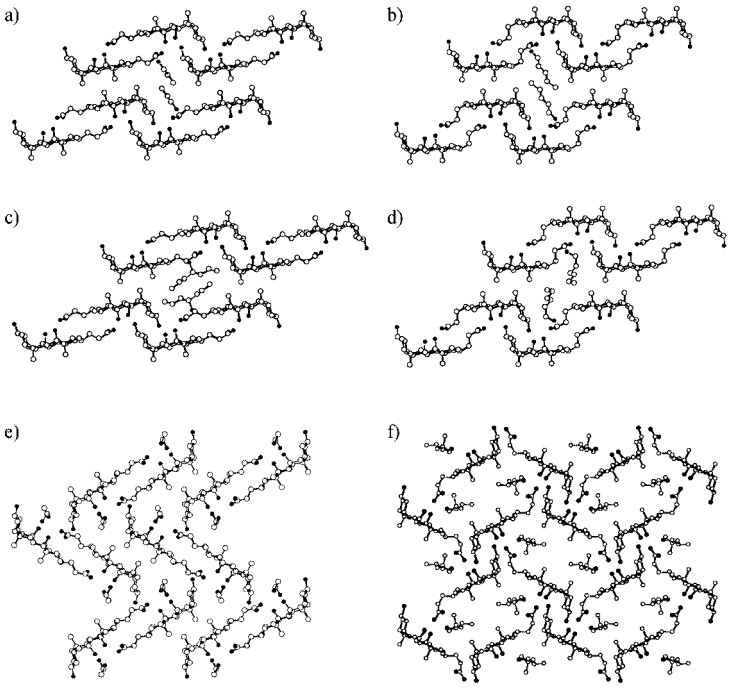

Figure 1. Molecular packing diagrams of a) CAM·**3** (α-*trans*), b) CAM·**15** (α-*gauche*), c) CAM·**39** (β-*trans*), d) CAM·**30** (β-*gauche*), e) CAM·**1** (herringbone), and f) CAM·**34** (crossing). Hydrogen atoms have been omitted for clarity; carbon, nitrogen, and oxygen atoms are represented by white, gray, and black circles, respectively.

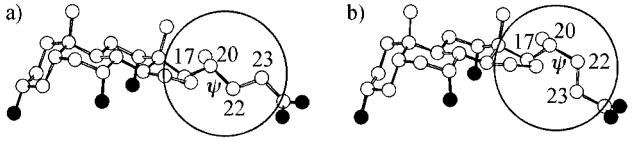

Figure 2. Conformations of the side chain: a) *trans* and b) *gauche*.

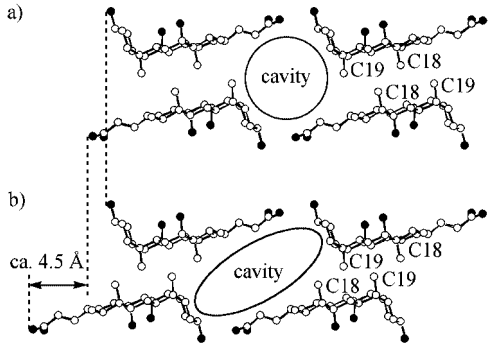

Figure 3. Interdigitation at the lipophilic face: a) α and b) β.

Herringbone Structure

Figure 1 (e) shows a herringbone structure, in which the three guest molecules **1**, **7**, and **48**, are included. The host framework has a one-dimensional cavity between the intersections of the layers, and the typical cross-sections of the cavities is shown in Figure 4 (e). Part d of Figure 5 shows a hydrogen-bond network that is a finite sequence of OH-[guest]···OH[C(7)]···OH[guest]···OH[C(12)]···O=C[C(24)]···

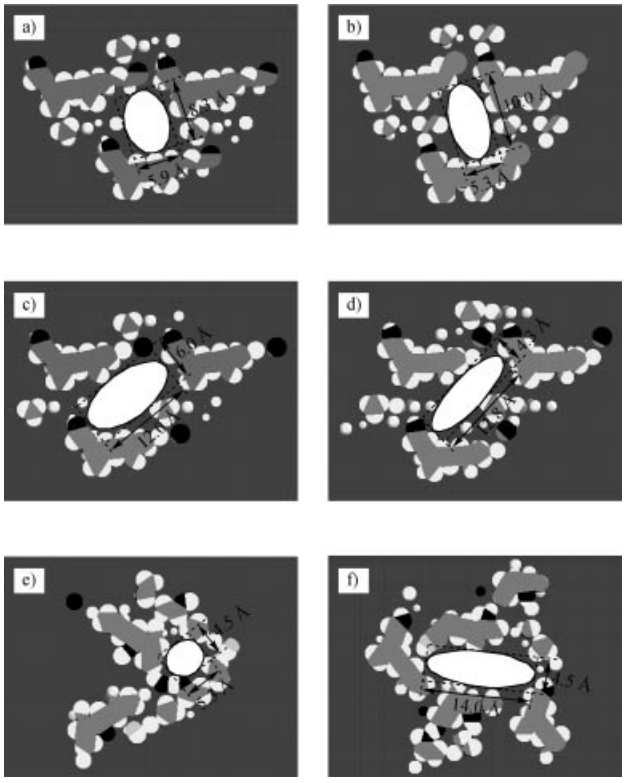

Figure 4. Cross-sections of the host channels sliced perpendicular to the direction of the channel of a) CAM·**3** (α-*trans*), b) CAM·**15** (α-*gauche*), c) CAM·**39** (β-*trans*), d) CAM·**30** (β-*gauche*), e) CAM·**1** (*herringbone*), f) CAM·**34** (*crossing*). Carbon, hydrogen, nitrogen, and oxygen atoms are represented in gray, white, light gray, and black, respectively; inclusion spaces are represented by circles.

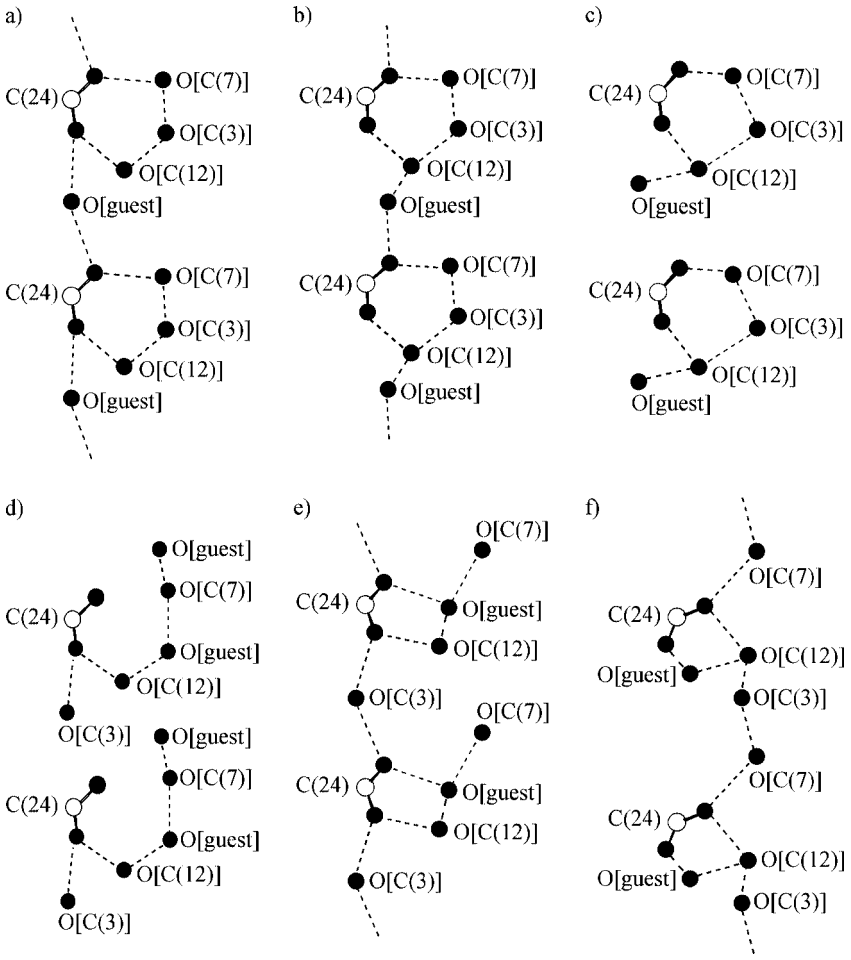

Figure 5. Hydrogen-bond networks in a) CAM·**3** (Type I), b) CAM·**9** (Type II), c) CAM·**39** (Type III), d) CAM·**1**, e) CAM·**7**, and f) CAM·**34**. Hydrogen atoms have been omitted for clarity; carbon, nitrogen, and oxygen atoms are represented by white, gray, and black circles, respectively.

OH[C(3)] in the crystal of CAM·**1**. In the case of **7** and **48**, the guest molecules participate in the cyclic hydrogen-bond network of the type ···OH[guest]···OH[C(12)]···O=C–NH_2[C(24)]···, as shown in part e of Figure 4. The adjacent cyclic networks are bridged by OH[C(3)], and OH[C(7)] weakly connects to the guest molecule in the cyclic network.

Crossing Structure

Figure 1 (f) shows the crossing structure that is observed in the inclusion crystal of **34**. The typical cross-section of the one-dimensional cavity is elliptical, as shown in part f of Figure 4. The structure has a different conformation of the side-chain from the other structures. Figure 5 (e) shows a cyclic hydrogen-bond network of the type ···OH[guest]···O=C–NH_2[C(24)]···OH[C(12)]···, which is bridged by OH[C(7)] and OH[C(3)].

Host Framework Isomerization

Since the isomerization of the host frameworks and the host/guest ratios are closely related with fitting in size between the guest molecules and the host cavity,[16a] the volume of the guest molecules and the host cavities was calculated, as summarized in Table 2. A wide range of guests (55.6–161.5 Å^3) can be included in bilayer structures that have the four sub-types. Although the molecular volumes of the present three guests **7**, **34**, and **48** (100.4–142.9 Å^3) are also suitable to the bilayer structures, they are not included in the bilayer structures but in the other two structural types. This suggests that the size of the cavity is not the sole factor that determines the isomerization of the host frameworks, and that other factors, such as shape and the host–guest hydrogen bond, also play an important role.

The host-framework isomerization of the sub-types in the bilayer structure can be understood in terms of guest size. In the case of 1:1 host/guest ratios, the three host frameworks α-*trans*, α-*gauche*, and β-*trans* tend to isomerize in the order with an increase in the volume of the included guest molecules; these volumes are in the ranges 73.1–107.8, 91.1–130.9, and 89.5–161.5 Å^3, respectively. Since a similar trend can be seen with 2:1 host/guest ratios, an increase of the guest volume causes a structural isomerization accompanied by a change in the host/guest ratios in the following order: α-*trans* (1:1), α-*gauche* (1:1), β-*trans* (1:1), α-*trans* (2:1), α-*gauche* (2:1), β-*trans* (2:1). This order agrees with that of the volumes of the host cavities in the three

Table 2. Host/guest ratio, molecular volume of guest, volume of cavity, number of guests in unit cell, and *PCcavity* in CAM crystals.

Guest	Host/guest molar ratio	V_{guest} [Å^3]	V_{cavity} [Å^3][a]	Number of guest molecules in unit cell	*PCcavity* [%][b]
Bilayer structure					
α-*trans type*					
2-Propanol (**4**)	1:1	73.1	288.5	2	50.6
1-Propanol (**3**)	1:1	73.4	274.3	2	53.5
2-Methyl-1-propanol (**5**)	1:1	90.3	300.3	2	60.1
2-Butanol (**9**)	1:1	90.5	316.9	2	57.1
1,2-Butandiol (**47**)	1:1	100.8	316.4	2	63.7
2,3-Butandiol (**49**)	1:1	100.8	322.8	2	62.5
(*S*)-2-Pentanol (**17**)	1:1	107.8	341.0	2	63.2
1,6-Hexanediol (**51**)	2:1	135.9	291.5	1	46.6
4,4-Dimethyl-2-pentanol (**33**)	2:1	142.9	286.5	1	50.0
1,7-Heptandiol (**52**)	2:1	153.7	279.0	1	55.1
2-Octanol (**41**)	2:1	161.2	299.1	1	53.9
α-*gauche type*					
1-Butanol (**8**)	1:1	91.1	316.3	2	57.6
3-Methyl-1-butanol (**11**)	1:1	107.7	349.5	2	61.6
1-Pentanol (**15**)	1:1	108.4	328.1	2	66.1
1,2-Pentandiol (**50**)	1:1	118.1	350.5	2	67.4
4-Methyl-1-pentanol (**22**)	1:1	124.6	385.0	2	64.7
4-Methylcyclohexanol (**55**)	1:1	130.9	373.9	2	70.0
1-Octanol (**40**)	2:1	161.8	320.1	1	50.5
1-Nonanol (**43**)	2:1	179.6	312.5	1	57.5
β-*trans type*					
Ethanol (**2**)	1:2	55.6	387.4	4	57.4
2-Methyl-2-propanol (**6**)	1:1	89.5	362.6	2	49.4
2-Methyl-2-butanol (**12**)	1:1	106.8	364.1	2	58.7
3-Methyl-2-butanol (**13**)	1:1	107.2	382.8	2	56.0
2,2-Dimethyl-1-propanol (**14**)	1:1	107.3	391.1	2	54.9
2-Methyl-1-butanol (**10**)	1:1	107.7	364.5	2	59.1
(*R*,*S*)-2-Pentanol (**18**)	1:1	107.8	356.2	2	60.5
(*R*)-2-Pentanol (**16**)	1:1	107.8	345.1	2	62.5
3-Pentanol (**19**)	1:1	108.1	388.9	2	55.6
3-Methyl-2-pentanol (**24**)	1:1	125.0	381.2	2	65.6
4-Methyl-2-pentanol (**25**)	1:1	125.0	382.0	2	65.4
2-Methyl-3-pentanol (**26**)	1:1	125.0	385.8	2	64.8
3,3-Dimethyl-1-butanol (**27**)	1:1	125.1	423.7	2	59.0
3,3-Dimethyl-2-butanol (**28**)	1:1	125.1	403.3	2	62.0
2-Methyl-1-pentanol (**20**)	1:1	125.5	386.2	2	65.0
3-Methyl-1-pentanol (**21**)	1:1	125.5	369.5	2	67.9
2-Methyl-2-pentanol (**23**)	1:1	125.5	385.0	2	65.2
2-Hexanol (**31**)	1:1	125.6	376.1	2	66.8
3-Hexanol (**32**)	1:1	125.9	385.1	2	65.4
2-Ethyl-1-butanol (**29**)	1:1	125.9	390.6	2	64.5
2-Methylcyclohexanol (**53**)	1:1	130.9	403.3	2	64.9
3-Methylcyclohexanol (**54**)	1:1	130.9	394.8	2	66.3
2-Methyl-1-hexanol (**35**)	1:1	143.3	402.3	2	71.2
2-Heptanol (**37**)	1:1	143.4	404.4	2	70.9
3-Heptanol (**38**)	1:1	143.7	413.0	2	69.6
4-Heptanol (**39**)	1:1	143.7	405.4	2	70.9
1-Heptanol (**36**)	1:1	144.0	404.3	2	71.2
2,5-Dimethylcyclohexanol (**56**)	1:1	148.7	406.2	2	73.2
3,4-Dimethylcyclohexanol (**57**)	1:1	148.7	393.9	2	75.5
3,5-Dimethylcyclohexanol (**58**)	1:1	148.7	441.9	2	67.3
3-Octanol (**42**)	1:1	161.5	431.3	2	74.9
5-Nonanol (**44**)	2:1	178.9	371.1	1	48.2
5-Decanol (**46**)	2:1	196.7	358.0	1	54.9
1-Decanol (**45**)	2:1	197.4	377.7	1	52.3
β-*gauche type*					
1-Hexanol (**30**)	1:1	126.2	366.1	2	68.9
Herringbone structure					
Methanol (**1**)	1:2	38.9	434.2	8	71.7
1-Methoxy-2-propanol (**7**)	1:1	100.4	696.8	4	57.6
1,4-Butandiol (**48**)	1:1	100.8	559.3	4	72.1
Crossing structure					
2,4-Dimethyl-3-pentanol (**34**)	1:1	142.9	989.0	4	57.8

[a] V_{cavity} is the volume of the cavity in the unit cell calculated with a 0.7 Å radius probe. [b] *PCcavity* is the packing coefficient of the guest molecules in the host cavity, given by the following expression: *PCcavity* [%] = [(V_{guest}) × (number of guest molecules in unit cell)]/V_{cavity} × 100.

host frameworks: the cavity volumes in α-*trans*, α-*gauche*, and β-*trans* are in the range of 274.3–341.0, 312.5–385.0, and 345.1–441.9 Å^3, respectively.

Packing Coefficients

The packing coefficient of the host cavities (*PCcavity*), which is the parameter that is used to estimate the steric fit between the guest molecule and the host cavity,[16a] can be derived from their volumes. As shown in Table 2, the *PCcavity* values of CAM inclusion crystals with aliphatic alcohols are in the range 46.6–75.5%, which is larger than those of the encapsulated host compounds in solution (46–64%)[18] and intermediate between the packing coefficients in the liquid state (44–56%)[18] and the crystalline state (66–77%).[19] Inclusion crystals out of this range would be difficult to form because of too close or loose packing between the guest molecule and the host cavity.

Figure 6 shows the relationship between the guest volumes and *PCcavity* in the three host frameworks α-*trans*, α-*gauche*, and β-*trans*, at 1:1 and 2:1 host/guest ratios. In the same host framework at the same host/guest ratio, *PCcavity* tends to increase with an increase of the guest volume. The plots of α-*trans* (1:1) and α-*gauche* (1:1) are located nearly on the same line (line I), and those of 2:1 host/guest ratios show a similar behavior (line III). The linear increase of *PCcavity* with the guest volume indicates that the two host frameworks can form cavities that are similar in size. The host framework isomerization from α-*trans* to α-*gauche* is therefore attributed not to size incompatibility between the guest molecule and the host cavity, but to the shape. The nearly round and elliptical cavities in α-*trans* and α-*gauche* types prefer guest molecules with shorter and longer alkyl chains, leading to the inclusion of smaller and larger alcohols, respectively.

On the other hand, the plots of β-*trans* (1:1) are located on the line of II, which is on the right side of line I. This indicates that this host framework has a larger host cavity than the α-*trans* and α-*gauche* types and that the host-framework isomerization from α-*gauche* to β-*trans* is driven by size fit. Moreover, the shape fit permits us to understand the selective formation of α-*gauche* and β-*trans* types for the middle-size guests (107–126 Å^3), which can be included in both host frameworks in the usual *PCcavity* range of 55–70%.[16a] Primary alcohols tend to be included in the α-*gauche* type, whereas secondary and/or branched alcohols are included in the β-*trans* type. Even though the former has the advantage of forming crystals with a higher *PCcavity*, the narrow cavity space around the amide group prevents the bulky alcoholic molecules from forming host–guest hydrogen bonds. As a result, the wider space in the β-*trans* type is suitable for bulky molecules, even though the resulting crystals have a lower *PCcavity*.

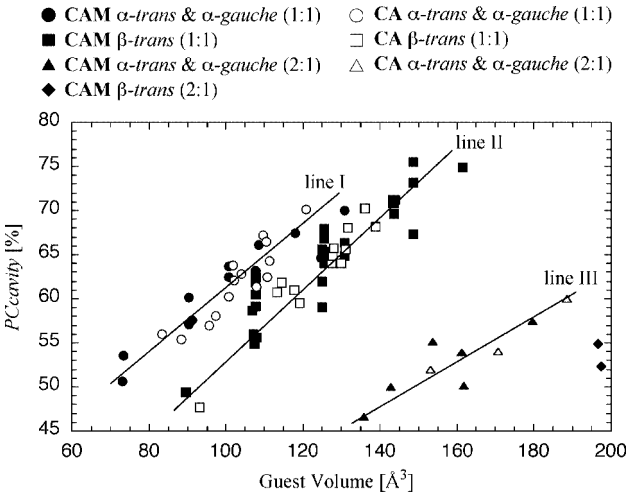

Figure 6. The relationship between guest volume and *PCcavity* in CAM and CA crystals.

Comparison with CA Host Framework

We have already reported the systematic investigation of CA crystal structures with aromatic guests.[16a] In this report, we revealed that CA forms bilayer structures in which three host framework types (α-*trans*, α-*gauche*, and β-*trans*) out of four types are ubiquitous, as in the case of CAM. Table 3 shows the average lattice parameters in the three types of CAM and CA crystals that belong to the $P2_1$ space group. In spite of the differences in the host and guest compounds, the lattice parameters in each type of the two hosts are very similar. Namely, CAM and CA form identical host frameworks with host cavities that are similar in shape and size. Figure 5 shows the relationship between the guest volumes and *PCcavity* of each type in CA crystals.[16a,16b] The plots of each type are located nearly on the lines corresponding to those in CAM. This indicates that the two hosts exhibit a similar behavior of the host-framework isomerization based on the guest size and shape.

Table 3. Average of lattice parameters in $P2_1$ crystals of CAM and CA.

Host	Framework type	Number of samples	*a* [Å]	*b* [Å]	*c* [Å]	*β* [°]	*V* [Å^3]	Ref.
CAM	α-*trans*	9	13.00	7.92	14.07	104.6	1402	this work
CA	α-*trans*	5	12.75	8.20	13.98	105.1	1409	[16a]
CAM	α-*gauche*	8	13.94	7.83	14.17	113.0	1422	this work
CA	α-*gauche*	20	13.65	8.10	14.10	114.2	1422	[16a]
CAM	β-*trans*	35	12.25	7.83	16.49	110.5	1481	this work
CA	β-*trans*	18	12.54	7.90	16.04	111.0	1474	[16a]

Table 4. Lattice parameters and host/guest ratio of inclusion crystals of CA with aliphatic alcohols.

Guest	Space group	*a* [Å]	*b* [Å]	*c* [Å]	*β* [°]	*V* [Å^3]	Host framework	Host/guest molar ratio	Ref.
Methanol	$P2_12_12_1$	15.20	11.63	14.56		2572	crossing	1:1	[20]
Ethanol	$P2_12_12_1$	14.65	11.74	15.05		2588	crossing	1:1	[21]
1-Propanol	$P2_12_12_1$	15.03	11.86	14.95		2655	crossing	1:1	[20]
2-Fluoroethanol	$P2_12_12_1$	14.59	15.32	11.79		2603	crossing	1:1	[22]
2,2-Difluoroethanol	$P2_12_12_1$	14.46	15.31	11.85		2623	crossing	1:1	[22]
2,2,2-Trifluoroethanol	$P2_12_12_1$	14.56	15.27	11.89		2645	crossing	1:1	[22]
1-Pentanol	$P2_1$	12.32	7.96	14.06	104.6	1336	α-*trans*	1:1	[16c]
1-Hexanol	$P2_1$	13.38	8.66	14.12	113.0	1506	α-*gauche*	1:1	[16c]

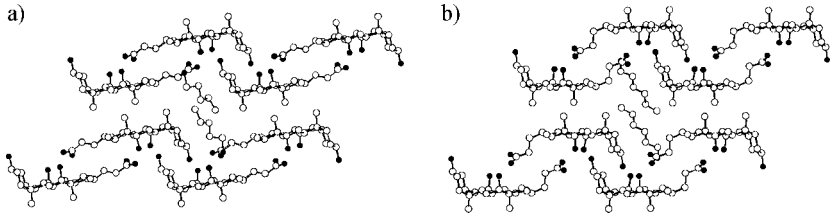

Figure 7. Molecular-packing diagrams of a) CA·**15** and b) CA·**30**.

In spite of the similarity of the host frameworks, the inclusion of aliphatic alcohols in CA crystals is in contrast to that in CAM. Recrystallization of CA from fifty or more alcohols results in the formation of only eight inclusion crystals. Moreover, only two alcohols are included in a bilayer structure,[16c] while another five smaller alcohols are found in a crossing structure.[20–22] Table 4 shows the lattice parameters of the inclusion crystals and the host framework types. The two alcohols − 1-pentanol and 1-hexanol − are incorporated in two host frameworks of the bilayer structures, as in the case of CAM. The host framework types, however, are different for the two hosts: 1-pentanol is found in CAM in an α-*gauche* type and in CA in an α-*trans* type, whereas 1-hexanol is found in CAM in a β-*gauche* type and in CA in an α-*gauche* type. Figures 7 and 8 show the crystal structures of CA with the two alcohols and the hydrogen-bond networks, respectively; the CAM crystal structures are shown in Figure 1. The difference in CAM and CA host frameworks with the same guests can be attributed to the formation of hydrogen-bond networks with the functional groups. The common feature of the hydrogen-bond networks in CAM bilayer structures is the bridge of the guest molecule that connects the adjacent host–host cyclic networks. When the amide changes to a carboxylic acid, however, this bridge is difficult to form due to the lack of a proton donor. The two inclusion crystals of CA with two alcohols have similar cyclic networks involving guest molecules. To form this network, the guest molecules need to penetrate deeper into the host layers than is the case in CAM. This is a plausible reason for the lack of formation of inclusion crystals of CA with secondary, tertiary, or branched-chain alcohols due to their steric repulsion. Furthermore, the inelasticity of the cyclic network in CA may also hinder the inclusion. In CAM crystals, two types of hydrogen-bond networks (I and II) can form depending on the guests in each host-framework type. This flexibility permits the guest molecules to be arrayed in the host cavity with less steric repulsion, leading to the inclusion of many more aliphatic alcohols.

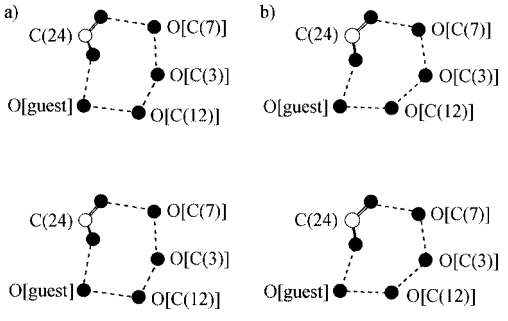

Figure 8. Hydrogen-bond networks in a) CA·**15** and b) CA·**30**.

Conclusions

We have described the systematic investigation of inclusion crystals of CAM with various aliphatic alcohols. Most of the crystals have a bilayer structure in which host-framework isomerization occurs depending on the size and shape of the guest molecules. The lattice parameters in each host-framework type and the behavior of the host-framework isomerization are very similar to those in bilayer crystals of CA. However, the inclusion of aliphatic alcohols in the two hosts is completely different because of the difference in host–guest hydrogen-bond networks with the functional groups of the host molecules.

There are many examples of host compounds that can form inclusion crystals with various organic guests through hydrogen-bonding and/or van der Waals interactions between the guests and the host molecules. Few hosts, however, can form identical host cavities in steric dimensions but different in their hydrogen-bond environment. There-

fore, this study is a good example of the importance of host–guest hydrogen bonds for guest inclusion.

Experimental Section

General Methods: All chemicals and solvents were commercially available and used without any purification. CAM was prepared by the conventional condensation reaction from CA and ammonia by the mixed anhydride method at –20 °C.[23] IR spectra were recorded on a JASCO IR-Report-100 or JASCO IR-810 spectrometer. Differential scanning calorimetry (DSC) and thermal gravimetry (TG) were performed on a Rigaku TAS100 system or Rigaku Thermoplus TG8120 with about 10 mg of sample from 40 to 230 °C at a heating rate of 5 °C min^{-1}. X-ray powder diffraction (XRD) patterns were measured with a Rigaku RINT-1100 diffractometer at room temperature.

Preparation of Inclusion Crystals: CAM (100 mg) was dissolved by warming in the liquid guest (usually 1–3 mL), and the resulting solution allowed to stand at room temperature. The obtained crystals were collected and dried on filter papers.

Crystal Structure Determinations: X-ray diffraction data were collected on a Rigaku AFC-7R four-circle diffractometer, a RAXIS-IV diffractometer, or a Rigaku R-AXIS RAPID diffractometer with 2D area detector with graphite-monochromated Cu-K_α or Mo-K_α radiation. Lattice parameters were obtained by least-squares analysis of 25 reflections measured in the range $20 < 2\theta < 25$ in the four-circle diffractometer and reflections for three oscillation images in the 2D area detector. Direct methods (SHELX-86, SIR-88, or SIR-92) were employed for the solution of the structure. The structure was refined by the full-matrix least-squares procedure with the program teXsan.[24] All non-hydrogen atoms were refined with anisotropic displacement parameters and hydrogen atoms of the host molecule were placed in idealized positions and refined as rigid atoms with the relative isotropic displacement parameters. The hydrogen atoms of the guest molecule were placed in idealized positions and no further refinement was applied. Many of the guest molecules with one or two chiral carbons showed disordered structures.[25] For example, the complexes with **13**, **20**, **21**, **24**, **26**, **33**, **46**, **54**, **56**, and **57** displayed highly disordered structures without an unambiguous assignment, while those with **7**, **18**, **25**, **31**, **35**, **37**, **38**, **41**, **47**, **50**, **53**, **55**, and **58** had a preferential isomer in their mixtures. The complexes with **28**, **32**, and **42** had two partly separated structures of their (*R*)- and (*S*)-isomers, while **9** and **10** had two separated ones. All calculations were performed using the teXsan crystallographic software package.
CCDC-189070–189093, -189098–189099, -189101–189107, -189109–189113, -189115–189128, -189131, -189133, -189136–189137, and -274798 contain the supplementary crystallographic data for this paper. These data can be obtained free of charge from The Cambridge Crystallographic Data Center via www.ccdc.cam.ac.uk/data_request/cif.

Calculations: The volumes of the guest molecules were calculated with Macromodel. The volumes of the host cavities were derived from the atomic coordinates by using the Free Volume program[26] in the Cerius^2 (version 4.0) software package.[27] The atomic radii [Å] adopted here are as follows: 1.20 for hydrogen, 1.70 for carbon, 1.65 for nitrogen, 1.60 for oxygen.

Supporting Information: (see footnote on the first page of this article) Tables S1 and S2, lattice parameters and torsion angles, and hydrogen bond lengths in CAM crystals.

Acknowledgments

This work was partially supported by Grants-in-Aid for Scientific Research (15350070) from the Ministry of Education, Culture, Sports, Science, and Technology, Japan. K. A. expresses his special thanks for the center of excellence (21COE) program "Creation of Integrated EcoChemistry of Osaka University".

[1] Reviews: a) D. D. MacNicol, J. J. McKendrick, D. R. Wilson, *Chem. Soc. Rev.* **1978**, *7*, 66–87; b) J. E. D. Davies, W. Kemula, H. M. Powell, N. O. Smith, *J. Inclusion Phenom.* **1983**, *1*, 3–44; c) *Top. Curr. Chem.*, vols. 140, 149 (Ed.: E. Weber), Springer-Verlag, London, UK, **1987**, **1988**; d) *Inclusion Compounds*, vols. 1–3 and 4–5 (Eds.: J. L. Atwood, J. E. D. Davies, D. D. MacNicol), Academic Press, London, **1984**, and Oxford Press, Oxford, **1991**; e) *Comprehensive Supramolecular Chemistry, Solid-State Supramolecular Chemistry: Crystal Engineering*, vol. 6 (Eds: D. D. MacNicol, F. Toda, R. Bishop), Pergamon, New York, **1996**; f) R. Bishop, *Chem. Soc. Rev.* **1996**, *25*, 311–319.
[2] a) P. Bhyrappa, S. R. Wilson, K. S. Suslick, *J. Am. Chem. Soc.* **1997**, *119*, 8492–8502; b) T. Tanaka, T. Tasaki, Y. Aoyama, *J. Am. Chem. Soc.* **2002**, *124*, 12453–12462; c) K. Biradha, D. Dennis, V. A. MacKinnon, C. V. K. Sharma, M. J. Zaworotko, *J. Am. Chem. Soc.* **1998**, *120*, 11894–11903; d) K. Kobayashi, T. Shirasaka, A. Sato, E. Horn, N. Furukawa, *Angew. Chem. Int. Ed.* **1999**, *38*, 3483–3486; e) S. V. Kolotuchin, P. A. Thiessen, E. E. Fenlon, S. R. Wilson, C. J. Loweth, S. C. Zimmerman, *Chem. Eur. J.* **1999**, *5*, 2537–2547; f) S. Kim, R. Bishop, D. C. Craig, I. G. Dance, M. L. Scudder, *J. Org. Chem.* **2002**, *67*, 3221–3230; g) V. A. Russell, C. C. Evans, W. Li, M. D. Ward, *Science* **1997**, *276*, 575–579.
[3] a) K. T. Holman, S. M. Martin, D. P. Parker, M. D. Ward, *J. Am. Chem. Soc.* **2001**, *123*, 4421–4431; b) K. T. Holman, A. M. Pivovar, J. A. Swift, M. D. Ward, *Acc. Chem. Res.* **2001**, *34*, 107–118.
[4] E. Weber, I. Csöegh, B. Stensland, M. Czugler, *J. Am. Chem. Soc.* **1984**, *106*, 3297–3306.
[5] M. D. Hollingworth, D. B. Santarsiero, K. D. M. Harris, *Angew. Chem. Int. Ed. Engl.* **1994**, *33*, 649–652.
[6] M. P. Byrn, C. J. Curtis, Y. Hsiou, S. I. Khan, P. A. Sawin, S. K. Tendick, A. Terzis, C. E. Strouse, *J. Am. Chem. Soc.* **1993**, *115*, 9480–9497.
[7] J. Bernstein, in *Organic Solid-State Chemistry*, vol. 32 (Ed.: G. R. Desiraju), Elsevier, Amsterdam, **1987**, pp. 471–518, and references cited therein.
[8] a) J. Bernstein, A. T. Hagler, *J. Am. Chem. Soc.* **1978**, *100*, 673–681; b) L. Yu, G. A. Stephenson, C. A. Mitchell, C. A. Bunnell, S. V. Snorek, J. J. Bowyer, T. B. Borchardt, J. G. Stowell, S. R. Byrn, *J. Am. Chem. Soc.* **2000**, *122*, 585–591.
[9] R. Thaimattam, F. Xue, J. A. R. P. Sarma, T. C. W. Mak, G. R. Desiraju, *J. Am. Chem. Soc.* **2001**, *123*, 4432–4445.
[10] B. Moulton, M. J. Zaworotko, *Chem. Rev.* **2001**, *101*, 1629–1658.
[11] D. Lawton, H. M. Powell, *J. Chem. Soc.* **1958**, 2339–2357.
[12] S. F. Aishahateet, K. Nakano, R. Bishop, D. C. Craig, K. D. M. Harris, M. L. Scudder, *CrystEngComm* **2004**, *6*, 5–10.
[13] M. Akazome, T. Takahashi, R. Sonobe, K. Ogura, *Tetrahedron* **2002**, *58*, 8857.
[14] Z. Urabanczyk-Lipkowska, F. Toda, in *Perspectives in Supramolecular Chemistry: Separations and Reactions in Organic Supramolecular Chemistry*, vol. 8 (Eds.: F. Toda, R. Bishop), John Wiley & Sons, Chichester, **2004**, pp. 1–31.
[15] a) K. Sada, T. Kondo, M. Miyata, T. Tamada, K. Miki, *J. Chem. Soc., Chem. Commun.* **1993**, 753–755; b) K. Sada, T. Kondo, M. Miyata, K. Miki, *Chem. Mater.* **1994**, *6*, 1103–1105; c) K. Sada, Y. Matsuura, M. Miyata, *Mol. Cryst. Liq. Cryst.* **1996**, *276*, 121–127; d) P. Briozzo, T. Kondo, K. Sada, M. Miyata, K. Miki, *Acta Crystallogr., Sect. B* **1996**, *52*, 728–733; e)

K. Sada, T. Kondo, M. Ushioda, Y. Matsuura, K. Nakano, M. Miyata, K. Miki, *Bull. Chem. Soc. Jpn.* **1998**, *71*, 1931–1937.
[16] a) K. Nakano, K. Sada, Y. Kurozumi, M. Miyata, *Chem. Eur. J.* **2001**, *7*, 209–220; b) N. Yoswathananont, K. Sada, M. Miyata, S. Akita, K. Nakano, *Org. Biomol. Chem.* **2003**, *1*, 210–214; c) N. Yoswathananont, K. Sada, M. Miyata, *Mol. Cryst. Liq. Cryst.* **2002**, *389*, 47–51; d) K. Nakano, K. Sada, M. Miyata, *Chem. Lett.* **1994**, 137–140.
[17] H. Nakano, *Molecular Graphics*, Science House, Tokyo, **1987**.
[18] S. Mecozzi, J. Rebek Jr., *Chem. Eur. J.* **1998**, *4*, 1016–1022.
[19] a) A. I. Kitaigorodskii, *Molecular Crystals and Molecules*, Academic Press, New York, **1973**; b) G. R. Desiraju, *Crystal Engineering: The Design of Organic Solids*, Elsevier, New York, **1989**; c) A. Gavezzotti, *Acc. Chem. Res.* **1994**, *27*, 309–314.
[20] E. L. Jones, L. R. Nassimbeni, *Acta Crystallogr., Sect. B* **1990**, *46*, 399–405.
[21] P. L. Johnson, J. P. Schaefer, *Acta Crystallogr., Sect. B* **1972**, *28*, 3083–3088.
[22] M. Shibakami, A. Sekiya, *J. Inclusion Phenom.* **1994**, *18*, 397–412.
[23] A. M. Bellini, M. P. Quaglio, M. Guarneri, G. Cavazzini, *Eur. J. Med. Chem.* **1983**, *18*, 185.
[24] teXsan, X-ray Structure Analysis Package; Molecular Structure Corporation, The Woodlands, TX, **1985**.
[25] For an example of disordered structures of guest molecules for inclusion compounds using nordeoxycholic aicd as a host, see: K. Kato, Y. Aoki, M. Sugahara, N. Tohnai, K. Sada, M. Miyata, *Chirality* **2003**, *15*, 53–59.
[26] R. Voorintholt, M. T. Kosters, G. Vegter, G. Vriend, W. G. J. Hol, *J. Mol. Graphics* **1989**, *7*, 243–245.
[27] *Cerius*^{2}, Molecular Simulation Software, Molecular Simulation Inc..

Received: June 15, 2005
Published Online: October 27, 2005

